

## High space resolution $\mu$ -RWELL for high particle rate

M. GIOVANNETTI, G. BENCIVENNI, G. FELICI, M. GATTA, G. MORELLO  
and M. POLI LENER

*INFN, Laboratori Nazionali di Frascati - Frascati, Italy*

received 8 June 2020

**Summary.** — The  $\mu$ -RWELL is a single-amplification stage-resistive MPGD. The amplification element is realized on a polyimide foil micro-patterned with high density blind-holes (wells) and is embedded through a thin resistive film in the readout PCB. The introduction of the resistive layer suppresses the transition from streamer to spark giving the possibility to achieve large gains ( $> 10^4$ ). As a drawback the capability to stand high particle fluxes is reduced. To avoid such a limitation different resistive layouts have been designed. The study of the performance of such layouts done at PSI, together with the measurement of the space resolution for orthogonal and inclined tracks performed at CERN are presented in this work.

### 1. – Introduction

The R&D on  $\mu$ -RWELL has two main purposes: the improvement of the stability in heavy irradiated environment while simplifying the construction procedures for an easy technology transfer to industry. The  $\mu$ -RWELL, fig. 1, is a resistive MPGD [1] composed of two elements: the cathode, a simple FR4 PCB with a thin copper layer on one side, and the  $\mu$ -RWELL\_PCB, the core of the detector. The  $\mu$ -RWELL\_PCB is composed of a wells matrix patterned Apical<sup>®</sup> foil acting as amplification element of the detector; a resistive layer, realized with a Diamond-Like-Carbon (DLC) film [2], as discharge limitation stage; a standard PCB, segmented as strip, pixel or pad electrodes, for readout purposes. The discharge suppression mechanism is similar to the one of the RPCs [3]: the streamer developed in the well, inducing a large current flowing through the resistive layer, generates a localized drop of the amplifying voltage with an effective quenching of the multiplication process in the gas. This mechanism suppressing the discharge amplitude allows to achieve large gains ( $> 10^4$ ) with a single amplification stage. As a drawback, the capability of the detector to stand high particle fluxes is reduced. A detector relying on this simple resistive layout suffers at high particle fluxes of a non-uniform response over its surface, that worsen as the size of the detector increases. In this paper we discuss the layouts for high rate purposes and their performance in terms of

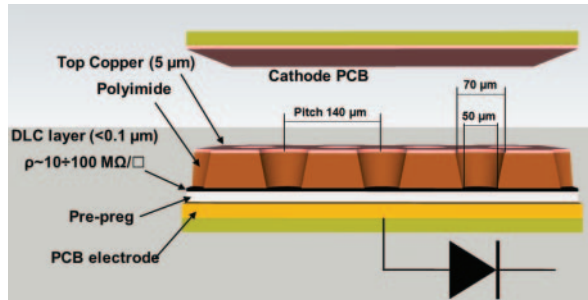


Fig. 1. – Layout of the  $\mu$ -RWELL.

efficiency and rate capability measured [4] at the  $\pi$ M1 beam line of the PSI. In addition we present the results of a study of the space resolution for orthogonal and inclined tracks performed at the CERN H8-SpS beam facility.

## 2. – The high rate layouts

The simplest scheme for the evacuation of the current in a  $\mu$ -RWELL is based on a single resistive layer with a grounding line all around the active area (Single Resistive Layout (SRL)), fig. 2. The path of the current to ground strongly depends on the incidence point of the particle. This problem can be overcome by introducing a high density grounding network on the resistive stage. Two different layouts with fast grounding have been implemented: the Double-Resistive Layout (DRL) with a 3-D grounding scheme and the Silver-Grid (SG) layout based on a single resistive layer with fast 2-D grounding.

**2.1. The double-resistive layout.** – The DRL layout is sketched in fig. 3. The first DLC layer is connected to a second DLC film by means of a matrix of conductive vias. A further matrix of vias connects the second DLC stage to the underlying readout electrodes, providing the grounding of the whole resistive stage. The vias density is typically  $<1 \text{ cm}^{-2}$ . In this way a sort of a 3D-current evacuation layout is implemented and the average resistive path to ground is minimized with respect to the SRL and the rate capability largely improved.

**2.2. The silver-grid layout.** – The silver-grid, fig. 4, is based on a single resistive layer with a thin conductive grid deposited on the DLC. The pitch of the grid together with the

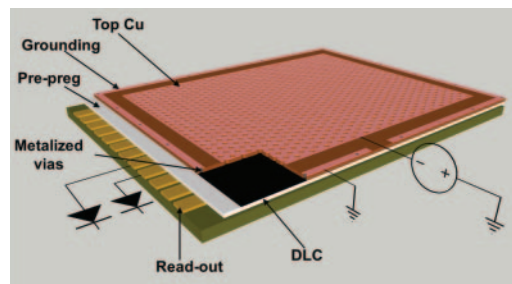


Fig. 2. – Sketch of the single resistive layout.

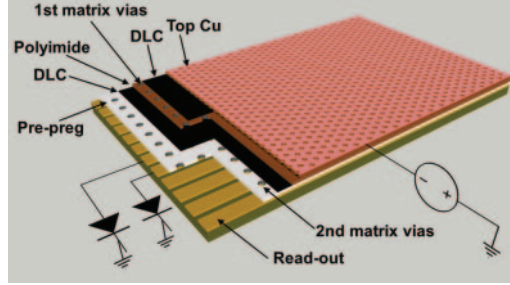


Fig. 3. – Sketch of the double-resistive layout.

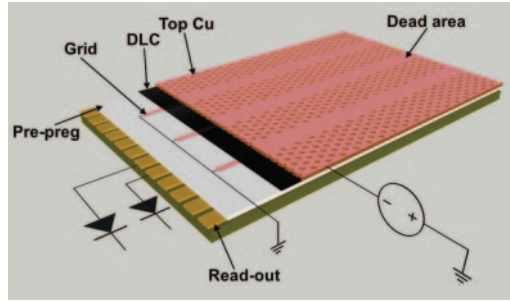


Fig. 4. – Sketch of the Silver Grid layout.

surface resistivity  $\rho$  of the DLC (hereafter simply called resistivity) are two parameters of this layout. Since the presence of a conductive grid on the DLC can induce discharges over the DLC surface, a small dead zone in the amplification stage above the grid lines has been inserted. In table I we report the characteristics of the SRL and the resistive layouts described in this work. The  $\Omega$  depends on the DLC resistivity and the geometrical parameters of the grounding scheme (*i.e.*, pitch, dead zone, etc). Under the assumption of a uniform particle flow irradiating the basic cell of the detector,  $\Omega$  represents the

TABLE I. – Resistive and current evacuation geometrical parameters of the HR layouts compared with the low rate baseline option (SRL).

Layout	$\rho$ ( $M\Omega/\square$ )	Pitch (mm)	Dead zone (mm)	Geom. acc. (%)	$\Omega$ ( $M\Omega$ )
SG1	70	6	2	66	134
SG2	65	12	1.2	90	209
SG2++	64	12	0.6	95	200
DRL	54	6	0	100	270
SRL	70	100	0	100	1947

average resistance seen by the current on the DLC:

$$(1) \quad \Omega = \frac{\rho (\text{pitch}/2 + \text{DOCA})}{2w},$$

where DOCA (*distance-of-closest-approach*) is the minimum distance between the grounding line and the closest well in the amplification element before the occurrence of a discharge on the DLC surface, and  $w$  is the unitary *transverse-width* of the resistive path of the current on the DLC film [4]. Due to the presence of a dead zone, the SG layouts exhibit a geometrical acceptance lower than the other layouts. For the SG2++ the dead zone has been minimized down to 5% of the active area.

### 3. – Performance of the HR layouts

The performance of the HR layouts has been measured at the  $\pi$ M1 of the PSI. A couple of plastic scintillators, providing the DAQ trigger, together with two external GEM trackers, defining the particle beam with a spatial accuracy of the order of  $100\ \mu\text{m}$  were placed upstream and downstream of six  $\mu$ -RWELL prototypes. The GEM have been equipped with  $650\ \mu\text{m}$  pitch X-Y strips, while the  $\mu$ -RWELL readout boards have been segmented with  $0.6 \times 0.8\ \text{cm}^2$  pads. All gaseous detectors, operated with an Ar/CO<sub>2</sub>/CF<sub>4</sub> (45/15/40) gas mixture, were read-out with APV25 front-end electronics [5].

**3.1. Efficiency studies.** – In fig. 5 the efficiency of the HR layouts is reported as a function of the detectors gain. The measurement has been performed with a 270 MeV/c  $\pi^-$  beam with a  $\sim 5 \times 5\ \text{cm}^2$  average beam spot (FWHM<sup>2</sup>). At a gain of 5000, the DRL, without dead zone, shows an efficiency larger than 98%, while the SG1 and SG2 achieve a detection efficiency of 78% and 95% respectively, larger than their geometrical acceptance. The SG2++, with a minimized dead zone, tends to an almost full efficiency of about 97%. The behaviour observed for the SG layouts, typical of detectors with GEM-like amplification stage [6], is correlated with the focusing effect on the primary ionization charge, resulting in a systematic reduction of the effective dead zone.

**3.1.1. Rate capability measurement.** The result of the rate capability study is shown in fig. 6, where the normalized gain of the HR layouts is reported as a function of the  $\pi$  flux.

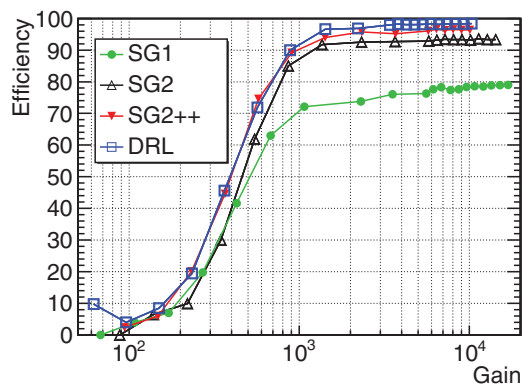


Fig. 5. – Efficiency as a function of the gas gain for the various HR layouts.

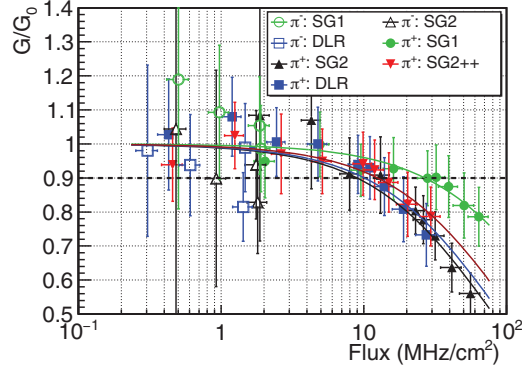


Fig. 6. – Normalized gas gain of the HR-layers as a function of the  $\pi^{+/-}$  flux at the  $\pi$ M1 facility of the PSI.

The detectors have been operated at a gain of about 5000. The low rate measurements have been performed with the  $\pi^-$  beam, while the high intensity behaviour has been studied with the  $\pi^+$  beam. The average beam spot was larger than the basic cell (pitch) of the HR layouts. The particle rate has been estimated with the current drawn by the GEM, that owns a linear behaviour up to several tens of  $\text{MHz}/\text{cm}^2$  [7]. The GEM have been operated at a gain of about 3500.

The gain drop observed at high particle fluxes is dominated by the Ohmic behaviour of the detectors due to the presence of the resistive film. In particular the HR layouts corresponding to  $\Omega \simeq 200 \text{ M}\Omega$  stand particle fluxes up to  $10 \text{ MHz}/\text{cm}^2$  with high detection efficiency.

#### 4. – Space resolution studies

For tracks orthogonal to the detector the space resolution is determined using two different methods: the Charge Centroid (CC) and the  $\mu$ -TPC mode. The Charge Centroid (CC) method uses the charge weighted strip centroid to reconstruct the track position on

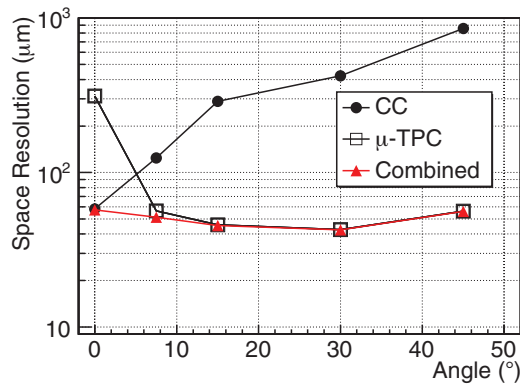


Fig. 7. – Space resolution of the  $\mu$ -RWELL. The angles are measured with respect to the perpendicular to the detector plane.

the readout plane, failing for inclined tracks or in presence of a high magnetic field giving a broad spatial distribution. The  $\mu$ -TPC mode, introduced by the ATLAS MicroMegas group [8], works better in cases exploiting the combined measurement of the time of arrival and the amplitude of the induced signals on the strip readout.

In fig. 7 we report the space resolution as a function of the track incidence angle. The detectors, equipped with a  $650\ \mu\text{m}$  pitch 1-D strip readout, were operated with an Ar/CO<sub>2</sub>/CF<sub>4</sub> (45/15/40) gas mixture at a gain of  $\simeq 8000$  and a drift field  $E_d = 0.5\ \text{kV/cm}$ . The CC (close circle) gives good results only for almost orthogonal tracks, while the  $\mu$ -TPC mode (open square) improves the space resolution for particles with large incident angle. Combining the two analysis methods (close triangle) an overall spatial resolution ranging between  $40\text{--}60\ \mu\text{m}$  is achieved.

## 5. – Conclusions

In this paper we have discussed different resistive layouts of  $\mu$ -RWELL for high rate applications. The prototypes have been tested up to particle fluxes exceeding  $20\ \text{MHz/cm}^2$  at the  $\pi\text{M1}$  beam facility of the PSI. A rate capability up to  $10\ \text{MHz/cm}^2$  with a detection efficiency of the order of 98% are the performance achievable with the proposed HR layouts. The SG2++ layout allows an easy technology transfer of the device to the industry operating in the field of multi-layer PCB. The detector, operated in combined CC/ $\mu$ -TPC mode, exhibits an excellent space resolution (down to  $40\ \mu\text{m}$ ) over a wide range of track incidence angles.

## REFERENCES

- [1] BENCIVENNI G. *et al.*, *JINST*, **10** (2015) P02008.
- [2] OCHI A. *et al.*, *PoS*, **TIPP2014** (2014) 351.
- [3] PESTOV Y. *et al.*, *Nucl. Instrum. Methods*, **93** (1971) 269.
- [4] BENCIVENNI G. *et al.*, *JINST*, **14** (2019) P05014.
- [5] RAYMOND M. *et al.*, *IEEE Nucl. Sci. Symp. Conf. Rec.*, **2** (2000) 9/113.
- [6] BENCIVENNI G. *et al.*, *Nucl. Instrum. Methods A*, **488** (2002) 493.
- [7] ALFONSI M. *et al.*, *Nucl. Instrum. Methods A*, **518** (2004) 116.
- [8] ALEXOPOULOS T. *et al.*, *Nucl. Instrum. Methods A*, **617** (2010) 161.